

Adversarial Diffusion Model for Unsupervised Domain-Adaptive Semantic Segmentation

Jongmin Yu^{a,b}, Zhongtian Sun^b, Shan Luo^{†c}

^a*ProjectG.AI, Yuseong-gu, Gajeong-ro 314-12, Daejeon, 34130, South Korea*

^b*Department of Applied Mathematics and Theoretical Physics, Centre for Mathematical Sciences, Wilberforce Rd, Cambridge, CB3 0WA, United Kingdom*

^c*Department of Engineering, King's College London, Strand, London, WC2R 2LS, United Kingdom*
Corresponding author: Shan Luo

Abstract

Semantic segmentation requires labour-intensive labelling tasks to obtain the supervision signals, and because of this issue, it is encouraged that using domain adaptation, which transfers information from the existing labelled source domains to unlabelled or weakly labelled target domains, is essential. However, it is intractable to find a well-generalised representation which can describe two domains due to probabilistic or geometric difference between the two domains. This paper presents a novel method, the Conditional and Inter-coder Connected Latent Diffusion (CICLD) based Semantic Segmentation Model, to advance unsupervised domain adaptation (UDA) for semantic segmentation tasks. Leveraging the strengths of latent diffusion models and adversarial learning, our method effectively bridges the gap between synthetic and real-world imagery. CICLD incorporates a conditioning mechanism to improve contextual understanding during segmentation and an inter-coder connection to preserve fine-grained details and spatial hierarchies. Additionally, adversarial learning aligns latent feature distributions across source, mixed, and target domains, further enhancing generalisation. Extensive experiments are conducted across three benchmark datasets-GTA5, Synthia, and Cityscape-shows that CICLD outperforms state-of-the-art UDA methods. Notably, the proposed method achieves a mean Intersection over Union (mIoU) of 74.4 for the GTA5 to Cityscape UDA setting and 67.2 mIoU for the Synthia to Cityscape UDA setting. This project is publicly available on <https://github.com/andreYoo/CICLD>.

Keywords: Diffusion model, adversarial learning, unsupervised domain adaptation, semantic segmentation

1. Introduction

Semantic segmentation, a fundamental task in computer vision, involves assigning labels to each pixel in an input image with high granularity. Over the past decade, significant efforts have been dedicated to advancing this field, leading to notable improvements through deep representation learning techniques [1, 2]. Competitions on major open benchmark datasets [3, 4, 5] have spurred the development of increasingly robust models; however, despite achieving new heights in benchmark performance, these models frequently face difficulties in real-world applications such as autonomous driving, which demand consistently high performance from the perception module. This discrepancy arises because benchmark datasets are typically biased towards specific environments, whereas real-world testing scenarios can present substantial domain variations due to factors like geographic location, lighting, camera differences, and weather conditions. Consequently, even highly advanced models can experience significant performance degradation in these situations, an issue that cannot be easily resolved by merely enhancing model complexity.

The most straightforward practical approach to enhancing a network’s generalisation capability is to gather and annotate data from a wider range of scenes. Nonetheless, densely annotating images is an arduous and labour-consuming process. For instance, in the Cityscapes dataset, [5], each image requires approximately 90 minutes to annotate. To address this limitation, researchers have developed methods to produce densely annotated images from rendered scenes efficiently, exemplified by the Synthia Dataset [4] and the Grand Theft Auto V (GTA5) Dataset [3]. However, the substantial visual disparity between simulated and real domains can markedly diminish the performance of models trained on synthetic data.

Due to these limitations, various domain adaptation methods have been developed to improve performance by exchanging information between data containing from diverse sources. Depending on the existence of labels in the domain for which performance is to be improved, domain adaptation can be classified as supervised [6, 7], semi-supervised [8, 9, 10, 11, 12, 13, 14], self-supervised [15], and unsupervised domain adaptation [16, 17, 18]. The purpose is to transfer information extracted from one domain to another domain. In this process, to improve the generalisation performance of the neural network itself, networks with various structures such as transformers [19] or spatial and channel attention mechanism [20] were used, and learning methods such as teacher-student learning were used [19, 15].

We tackle the intricate problem of unsupervised domain adaptation (UDA) in

semantic segmentation. We aim to transfer a segmentation model trained on a labelled source domain to an unlabeled target domain devoid of predefined supervision. Given that UDA operates under the assumption of absent-label information in the target domain [21], it presents a notably more intricate challenge compared to other domain adaptation scenarios [22]. To solve the UDA, a segmentation model should be well-generalised for the source domain, and the model could be well-transferred to a model for a target domain. Until recently, research was conducted to apply various network structures and add various objective functions to improve generalisation performance [16, 17, 18, 19, 15].

Addressing the challenge of UDA, we present a semantic segmentation model using a diffusion model and unsupervised domain adaptation based on adversarial learning. Diffusion models [23, 23, 22], known for their capability to generate high-quality, diverse samples and learn complex data distributions, can be considered a novel approach to overcome these limitations. The proposed method, based on the diffusion model’s intrinsic ability to model the gradual transition between different domains, can produce more generalised and accurate feature representations. These advantages are well-matched with the challenging issue for the UDA for semantic segmentation.

Our method employs a self-training-based learning framework, wherein the model predicts the target domain and subsequently uses these predictions to update itself. We develop a segmentation model employing a diffusion-based methodology, which is trained on a source domain and adeptly extrapolated to predict a target domain. The segmentation using our diffusion-based method can be considered a mapping function, including the diffusion process (noising and denoising processes) on the latent feature space between an image and a segmentation mask. During the denoising process, We apply a conditioning module using a segmentation mask to improve semantic information on the latent features. In order to transfer the source domain’s information to the model for the target domain, we formulate adversarial learning aiming to adapt by confusing the domain discriminator, maintaining domain alignment separate from task-specific learning under distinct losses.

The contributions of this paper are threefold. First, we propose a novel conditional and inter-coder connected latent diffusion (CICLD) based on semantic segmentation. The CICLD contains a long skip-connection to explicitly bridge information between each encoder and decoder pair and also enrich the semantic information by applying the conditioning module during the diffusion process. The proposed CICLD can learn more generalised representation from a given source domain so that, consequently, it will improve the segmentation performance on the target domain.

Second, we present adversarial learning to improve the domain adaptation performance on CICLD. The formulated adversarial learning is applied to the denoising process on the latent diffusion model, and it adversarially classifies the denoised latent features of source and target domains. This adversarial learning approach effectively aligns the feature distributions between the source and target domains, leading to improved domain adaptation capabilities and consequently improving the generalisation performance for domain adaptation.

Third, we demonstrate the effectiveness of our proposed methodology through extensive ablation studies and comparisons with state-of-the-art methods. In our experiments, the CICLD achieves state-of-the-art performance on two challenging unsupervised domain adaptation benchmarks. Specifically, it attains 74.4 mIoU and 67.2 mIoU for the GTA5→Cityscape and Synthia→Cityscape UDA settings, respectively, surpassing the performance of existing state-of-the-art UDA methods. These results highlight the superior domain adaptation capabilities of the CICLD and its potential to bridge the gap between source and target domains in semantic segmentation tasks.

The structure of this paper is as follows: Section 2 reviews related works and offers a foundational overview of diffusion models. Section 3 details our proposed approach for Unsupervised Domain Adaptation (UDA) in semantic segmentation. Section 4 provides comprehensive information on the experimental setup and discusses the results. The paper concludes with Section 7, summarising key findings and implications.

2. Related works

2.1. Semantic segmentation

Semantic segmentation is a fundamental task in computer vision that involves classifying each pixel in an image into a predefined category. This fine-grained classification is essential for various applications, including autonomous driving [24], medical imaging [25, 26], and scene understanding [27]. Recent advancements in this field have been significantly influenced by the development of deep learning, particularly convolutional neural networks (CNNs) [28]. However, recently, the landscape of semantic segmentation has evolved with the introduction of novel approaches such as transformers [27, 24, 26, 29, 22], self-supervised learning [30, 31], and diffusion models [32, 33, 22]. Each of these methods brings unique advantages and challenges, contributing to the rich diversity of the current state-of-the-art in semantic segmentation.

Transformers have revolutionised natural language processing and have recently made significant strides in computer vision tasks, including semantic segmentation. Methods like Segmenter [27], SegFormer [24], and TransUNet [26] leverage the ability of transformers to capture global context and dependencies, which are crucial for accurate segmentation. For instance, Segmenter [27] uses vision transformers to model long-range dependencies, effectively enhancing segmentation performance. SegFormer [24] simplifies the transformer architecture, making it efficient and effective for segmentation tasks. TransUNet [26] combines transformers with the UNet architecture [25], specifically improving performance in medical image segmentation. The main advantage of these methods is their superior ability to capture global context, leading to improved accuracy. However, they often come with increased computational complexity and higher memory requirements than traditional CNN-based approaches.

Self-supervised learning (SSL) has emerged as a powerful paradigm, especially when labelled data is scarce. Since *et al.* [31] focus on learning representations from unlabelled data to predict. These approaches are advantageous because they reduce the dependency on large annotated datasets, which are often expensive and time-consuming. As a result, their method significantly improves performance in medical image segmentation by leveraging dense self-supervised learning techniques. The primary benefit of SSL methods is their ability to generalise well across different domains and tasks. However, they can sometimes fall short in scenarios where the pretext tasks do not align well with the downstream segmentation tasks, potentially leading to sub-optimal feature representations.

Recently, diffusion models [32, 33] have shown promise in generative modelling, and their application to semantic segmentation is gaining traction. Denoising Diffusion Implicit Model [33] demonstrates high-quality image generation capabilities, which can be directly applied to segmentation tasks. The primary advantage of diffusion models is their ability to generate detailed and accurate segmentation maps, leveraging their generative capacities. However, applying diffusion models for the semantic segmentation is just beginning [22, 34, 35, 36, 37]. Baranchuk *et al.* [34] and Tan *et al.* [35] applied the diffusion process to generate multi-scale latent features for image segmentation. Wu *et al.* [36] leveraged a diffusion-based text-to-image generation approach to generate semantic segmentation results. Those approaches leverage the outstanding sampling capacity of diffusion models for semantic segmentation and assume that the training dataset is large-scale and well-organised. In this work, we propose a semantic segmentation method based on the diffusion model and apply it to unsupervised domain adaptation. The continued evolution and diversification of approaches promise to drive further improvements

in semantic segmentation, making it an exciting topic of research and application.

2.2. Unsupervised domain adaptation

Unsupervised Domain Adaptation (UDA) entails training a model to transfer knowledge from a domain with available labels to a domain without annotations [19]. Recently, UDA techniques for semantic segmentation have seen significant advancements through the use of data augmentations [38, 39], feature alignments [40, 22], and self-supervised learning [19, 20]. Traditionally, these methods have leveraged synthetic datasets like GTA5 [3] or Synthia [4] as the labelled source domain, transferring knowledge to real-world datasets such as Cityscapes in the unlabelled target domain. These conventional benchmarks are reasonable because making a synthetic segmentation dataset is way easier than labelling real images. However, it is obvious that context information, such as texture and object variations of synthetic images and real images, are very different. This context information gap makes learning highly generalised representations from synthetic images very important.

It is widely recognised that the generalised representational power of a segmentation model often does not translate effectively across domains, leading to inferior cross-domain performance. Consequently, domain adaptation for semantic segmentation has become a highly active area of research. Various adaptation methods have been introduced, including adversarial training at the input image level [39], feature level [16, 39], and network output level [17]. For instance, Hoffman *et al.* [39] seek to mitigate the domain gap by first converting source images to the target style using a cycle consistency loss, followed by aligning cross-domain feature distributions through adversarial training. Additionally, Saito *et al.* [40] propose a method to identify non-discriminative samples near decision boundaries using a critic network, enabling the generator to produce more discriminative features by deceiving the critic network with adversarial training. Zhang *et al.* [41] introduced a curriculum adaptation method to regularise the predicted label distributions in the target domain, ensuring they align with the label distributions in the source domain.

To improve the semantic segmentation model’s representation performance and consequently the unsupervised domain adaptation’s result, we have designed a diffusion model-based semantic segmentation model and formulated an adversarial learning-based unsupervised domain adaptation. Our diffusion-based method can learn more generalised and outstanding representations from synthetic images and convey representational information for the target domain via adversarial learning.

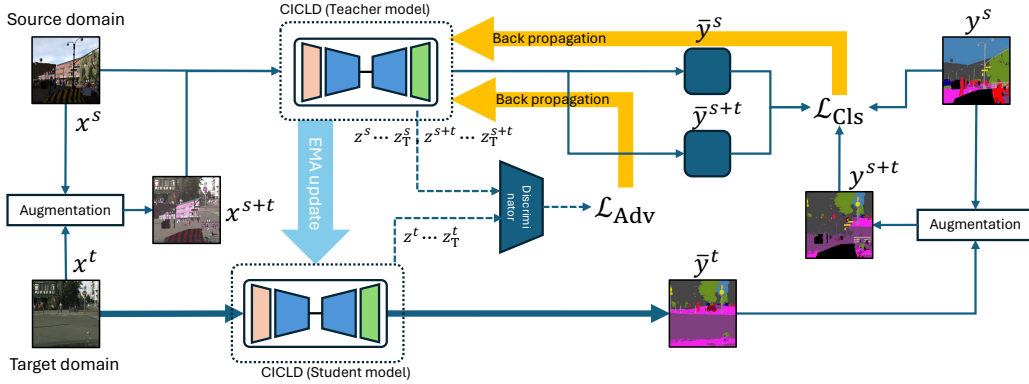


Figure 1: Illustration of workflow details for pre-training, fine-tuning, and inference processes of the unsupervised domain adaptation using CLDM for semantic segmentation. The dotted lines denote the adversarial learning process. The bolded lines define the workflow of the CLDM for segmentation in the test step.

3. The proposed method

3.1. Preliminaries

The goal of diffusion models [23] is to find the parameterised data distribution $p_\theta(\mathbf{x}_0)$ using a given data $\mathbf{x}_0 \sim q(\mathbf{x}_0)$. To do this, when a data \mathbf{x}_0 is given, the training of diffusion models conducts a *forward process* (a.k.a. diffusion process) $q(\mathbf{x}_t|\mathbf{x}_{t-1})$, which adds Gaussian noise to the data and a *reverse process* (a.k.a. denoising process) $p_\theta(\mathbf{x}_{t-1}|\mathbf{x}_t)$, which denoises the given noised data by subtracting predicted noise.

The forward process $q(\mathbf{x}_t|\mathbf{x}_{t-1})$ is a task to add Gaussian noise to data at a certain time step $t \leq T$. The Gaussian noise is generated by a Gaussian probability $\mathcal{N}(\cdot)$ with scheduled variance: β_1, \dots, β_T . The entire forward process to generate completely noised sample \mathbf{x}_T is represented by

$$\begin{aligned}
 q(\mathbf{x}_{1:T}|\mathbf{x}_0) &:= \prod_{t=1}^T q(\mathbf{x}_t|\mathbf{x}_{t-1}), \\
 q(\mathbf{x}_t|\mathbf{x}_{t-1}) &:= \mathcal{N}(\mathbf{x}_t; \sqrt{1 - \beta_t}\mathbf{x}_{t-1}, \beta_t\mathbf{I}).
 \end{aligned} \tag{1}$$

The reverse process $p_\theta(\mathbf{x}_{t-1}|\mathbf{x}_t)$ can be considered as a denoising task. For each time step t , a diffusion model predicts a noise and subtracts it from the noised data. This task is represented by Markov Chain so that it can be represented by

parametric conditional distribution, as follows:

$$\begin{aligned}
 p_\theta(\mathbf{x}_{0:T}) &:= p(\mathbf{x}_T) \prod_{t=1}^T p_\theta(\mathbf{x}_{t-1}|\mathbf{x}_t), \\
 p_\theta(\mathbf{x}_{t-1}|\mathbf{x}_t) &:= \mathcal{N}(\mathbf{x}_{t-1}; \boldsymbol{\mu}_\theta(\mathbf{x}_t, t), \boldsymbol{\Sigma}_\theta(\mathbf{x}_t, t)).
 \end{aligned} \tag{2}$$

The learning of the diffusion model is to find the suitable parametric distribution $p_\theta(\mathbf{x}_0)$ representing a given data. This distribution is central to reconstructing the original data from its noised state. However, directly optimising the negative log-likelihood of $p_\theta(\mathbf{x}_0)$ poses computational challenges due to its complexity. Consequently, optimisation is conducted via a variational lower bound, which is more computationally feasible and is formulated as follows:

$$\begin{aligned}
 L_{dm} &:= \mathbb{E}[-\log p_\theta(\mathbf{x}_0)] \leq \mathbb{E}_q \left[-\log \frac{p_\theta(\mathbf{x}_{0:T})}{q(\mathbf{x}_{1:T}|\mathbf{x}_0)} \right] \\
 &= \mathbb{E}_q \left[-\log p(\mathbf{x}_T) - \sum_{t \geq 1} \log \frac{p_\theta(\mathbf{x}_{t-1}|\mathbf{x}_t)}{q(\mathbf{x}_t|\mathbf{x}_{t-1})} \right].
 \end{aligned} \tag{3}$$

In DDPM [23], it found that the forward and reverse processes are represented by reparameterisation tricks; therefore, it can be replaced by the minimisation of prediction error for a Gaussian noise and noise prediction obtained by a neural network. As a result, Eq. 3 is further simplified to the l_2 -distance between the generated Gaussian noise $\epsilon \sim \mathcal{N}(\mathbf{0}, \mathbf{I})$ and predicted noise ϵ_θ at a certain time step. Using the notations, $\alpha_t := 1 - \beta_t$ and $\bar{\alpha}_t := \prod_{s=1}^t \alpha_s$, the simplified loss is represented by

$$\mathbb{E}_{\mathbf{x}_0, \epsilon} \left[\frac{\beta_t^2}{2\sigma_t^2 \alpha_t (1 - \bar{\alpha}_t)} \left\| \epsilon - \epsilon_\theta(\sqrt{\bar{\alpha}_t} \mathbf{x}_0 + \sqrt{1 - \bar{\alpha}_t} \epsilon, t) \right\|^2 \right]. \tag{4}$$

3.2. Methodology overview

Fig. 1 provides our proposed approach’s structural details and loss functions. For unsupervised domain adaptation, the input to our model is a source image x^s and a target image x^t sampled from the source and target distributions, respectively. We subsequently create a mixed image x^{s+t} , where the source and target images are mixed using the approach in ClassMix [42]. Here, source pixels belonging to randomly sampled classes are overlaid on the target image, and pixel-level augmentations are applied to the resulting mixed image. The same module is applied in the labels as well; however, the UDA task operates under the assumption

of absent-label in the target domain during the training phase to generate the pseudo labels y^{s+t} for the x^{s+t} . In generating the pseudo label, the predicted labels \bar{y}^t by a student model (See Fig. 1) are used.

Those images pass through the teacher model parts. A sample of the source domain x^s is encoded to the corresponding latent feature z_0^s using the encoder \mathcal{E} , and it proceeds via the diffusion process (Eq. 1) to generate noised latent feature z_T^s and denoising process (Eq. 2) using the UNet ϵ_θ to obtain denoised latent feature \bar{z}_0^s (refer to Fig. 2). During those diffusion processes, the corresponding labels y^s and y^{t+s} are used as conditional signals c in enriching the semantic information while the latent features are transferred to generate segmentation results. The conditional signal is obtained by extracting the latent features from the segmentation labels using additional pre-trained neural network f_{mask} (See Fig. 2). After that, the denoised latent feature is applied to the decoder \mathcal{D} and the fully connected network f_{cls} to generate the pixel-level class map \bar{y}^s (illustrated in Fig. 2). The above process applies to the mixed image x^{s+t} . The predicted segmentation results \bar{y}^s and \bar{y}^{s+t} are applied to compute the cross-entropy loss \mathcal{L}_{cls} (Eq. 7) and back-propagate to update the teacher model parameters.

The information of the target domain can be obtained while the model is optimised by the cross-entropy loss using the mixed samples x^{s+t} and the corresponding label y^{t+s} . However, it is obviously beneficial to apply the loss term for an explicit domain adaptation. We additionally apply an adversarial loss to explicitly align the distribution of latent features for the source and target domains to improve the generalisation performance of the UDA. It conducts adversarial learning between the latent feature spaces of the source domain, mixed domain, and target domains. In particular, adversarial learning collaborates with the diffusion process so that adversarial learning loss is computed for every denoising step and will consequently be averaged for each batch. The gradient of the adversarial loss is back-propagated to the Unet ϵ_θ for the denoising process to improve the generalisation performance in the denoising process. Moreover, as with the classification loss, the computed gradient is applied to the teacher model only. The student model, serving as the segmentation model for the target domain, is updated using the Exponential Moving Average (EMA) algorithm to ensure stability and improve generalisation during the domain adaptation process [19] In the inference step, the student model is used for the testing.

3.3. Architectural details of CICLD

Several studies have been presented that apply diffusion models for semantic segmentation [34, 35, 36, 37]. However, those approaches still face challenges

in computational complexity since those studies applied diffusion models to the high-dimensional data space. To reduce the computational complexity and improve the flexibility in embedding other complementary information, such as a mask or vector-embedded prompt, Rombach *et al.* [43] proposed the latent diffusion model (LDM), which moves in developing the CICLD. In semantic segmentation, Amit *et al.* [37] present a diffusion model for the segmentation task, which uses a latent feature encoded from an image to improve the segmentation performance.

The architectural framework of the CICLD incorporates similar core components such as an encoder and decoder structures for compressing high-dimensional data. A key structural distinction compared with Rombach *et al.* [43] is the inter-coder connection—a long-skip connection between the encoder and decoder. This structural innovation enhances feature transfer and integration, significantly improving semantic segmentation by preserving detailed spatial and contextual information. Additional details on the conditioning mechanisms and the specific configuration of these connections will be discussed later.

Conditioning: As shown in Fig. 2, the conditional signal c is applied while the denoising process is being conducted using the UNet ϵ_θ , and this can be interpreted that the diffusion model will be optimised with the conditioning task $p(z|c)$ to improve the contextual property of transferring the latent feature extracted from the image to predict the semantic segmentation results. We embedded the conditioning vector to the UNet ϵ_θ to compile this conditioning task. This can be implemented with a conditional denoising autoencoder $\epsilon_\theta(z_t^*, t|c^*)$, where $z^* \in \{z^s, z^{s+t}\}$ is a latent feature extracted from the source and mixed image domains and c^* defines the corresponding conditioning vector that is also extracted from the source y^s and mixed y^{s+t} domains’ labels. In extracting the conditioning vectors from the labels, we use a mask encoder f_{mask} , which is an independent neural network model trained by ImageNet dataset [44].

The conditioning operation in the UNet is accomplished by using the attention mechanism. After computing the self-attention vector between the latent feature of U-Net and the conditioning vector, the conditioning is done by conducting the element-wise summation between the two vectors, which is represented as follows:

$$\hat{o}_t^* = o_t^* + \sigma(o_t^* c') c \quad (5)$$

where o_t^* is the feature extracted from the middle layer of the UNet ϵ_θ for t^{th} noised latent feature. It can be defined as o^s or o^{s+t} , which are the features extracted from the source domain and the mixed domain, respectively. \hat{o}_t^* is conditioned features. c' denotes that the conditional vector is transposed before it is multiplied

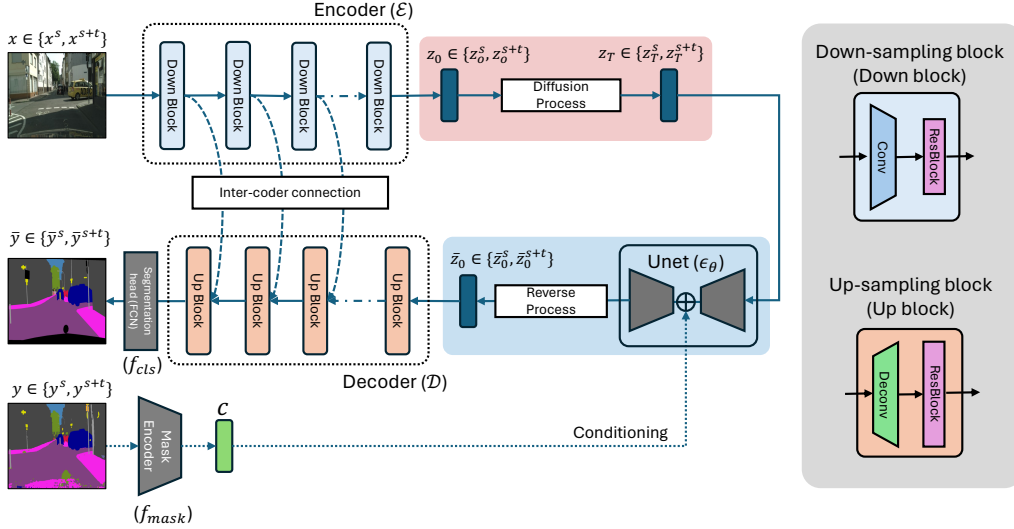


Figure 2: Architectural details of the conditional and inter-coder connected latent diffusion (CICLD). During the training phase, x can be defined by the source and target domain images x^s and x^{s+t} . Depending on the given domain, the latent features (z_0 and z_T , and \bar{z}_0), the mask y , and the output \bar{y} can be noted by the source domain’s one ($z_0^s, z_T^s, \bar{z}_0^s, y^s$, and \bar{y}^s) or the mixed domains’ one ($z_0^{s+t}, z_T^{s+t}, \bar{z}_0^{s+t}, y^{s+t}$, and \bar{y}^{s+t}), respectively.

with feature. The conditioned feature is applied to the remaining networks in ϵ_θ to generate the \bar{z}_0 , which is a denoised and transferred feature for predicting semantic segmentation results.

By conditioning on segmentation masks during training, the diffusion model learns to capture the complex boundaries and structures associated with different classes within the images. This results in a more refined understanding of object shapes, sizes, and spatial relationships, which can significantly improve the accuracy of the segmentation. Also, conditioned training enforces contextual integrity by ensuring that the generated segments make sense within the broader context of the image. For instance, the model learns not to segment parts of an object as separate from the whole merely based on colour or texture variations, which might confuse less context-aware segmentation methods. To demonstrate the effectiveness of the conditioning, we conducted an ablation study.

Inter-coder connection: We built the skip connection structure between the encoder \mathcal{E} and the decoder \mathcal{D} (See Fig. 2, sparsely dotted line between the encoder and the decoder). The concept of the long skip-connection was seldom discussed in

several previous works [45, 46]. Those works define the long skip connection as a connection between a complex network module such as a residual block in ResNet [2] or sparse connected architecture in InceptionNet [47], and experimentally show that the long skip-connection is helpful in keeping the semantic and contextual information when input images are up or down-sampled and alleviate vanishing gradient.

The LDM has long skip connections in its UNet structure. This only influences the denoising performance since the connection is only built inside the UNet. Even if the latent feature denoised by the UNet is conditioned by the segmentation mask vector, which enhances the semantic context, it may not be detailed enough, in particular, to distinguish the object boundaries because that conditioning will not affect up-sampling by the decoder. Several semantic segmentation methods overcome this issue by using skip-connection structures. Still, LDM does not employ skip-connection between the encoder and the decoder except for the skip-connection in the UNet for denoising.

In semantic segmentation, finding object boundaries is one of the important, challenging issues; therefore. To solve this issue, we build the inter-coder connection, which is a skip-connection structure between the encoder \mathcal{E} and the decoder \mathcal{D} . Unlike the LDM having the skip connection structure in the UNet only, the inter-coder connection directly generates information flow between the encoder and the encoders, which was actually disconnected by the UNet.

By connecting the encoder and decoder, the model can transfer fine-grained details and spatial hierarchies directly across the network, helping to preserve details that are often lost during the encoding process. This is particularly beneficial for distinguishing object boundaries, where maintaining texture and detail fidelity is crucial. Additionally, for a semantic segmentation task that requires precise spatial information, direct paths from the encoder to the decoder ensure that spatial relationships and contextual information are effectively utilised and maintained throughout the generation process. We conducted ablation studies to empirically validate the effectiveness of the inter-coder connection in Section 5.2.

3.4. Training objectives

Conditional LDM loss: We reformulate the diffusion loss function in the DDPM [23] to apply the diffusion process to the latent feature space. The loss function is used to optimise the Unet f_{Unet} only by minimising given noise ϵ and the predicted noise by the Unet $\bar{\epsilon}$. The loss function for the diffusion process is formulated as

follows:

$$\arg \min_{f_{\text{Unet}}} L_{\text{Dif}}(t, z^*, \epsilon) = \|\epsilon - \epsilon_{\theta}(\sqrt{\bar{\alpha}_t}z^* + \sqrt{1 - \bar{\alpha}_t}\epsilon, t)\|^2, \quad (6)$$

where z^* can be defined by the latent features for the source image z^s , mixed image z^{s+t} , and target image z^t . α is defined by the scheduled variance. For further details, please refer to the DDPM [23].

Classification loss: We have chosen the standard softmax cross-entropy formula to serve as our classification loss, which is defined as follows:

$$\arg \min_{\mathcal{E}, \mathcal{D}} \mathcal{L}_{\text{Cls}}(\bar{y}^*, y^*) = \mathbb{E}[y^* \log(\bar{y}^*)], \quad (7)$$

where \bar{y}^* can be defined by predicted segmentation results \bar{y}^s and \bar{y}^{s+t} , and y^* can be defined by image labels y^s and y^{s+t} .

Adversarial loss: The adversarial loss is applied to improve the generalisation performance for the unsupervised domain adaptation explicitly. A typical adversarial loss is related to distinguishing whether an input is generated by a generator or a given true sample. Hence, it is basically a two-class classification problem. In this work, we formulate adversarial loss for the three-class classification using softmax cross entropy and Kullback-Leibler (KL) divergence. The adversarial loss is formulated as follows:

$$\begin{aligned} \arg \min_{\mathcal{E}} \max_{f_{\text{dis}}} L_{\text{Adv}}(z^*) &= \underbrace{\mathbb{E}[o^* \log(f_{\text{dis}}(z^*))]}_{\text{For } f_{\text{dis}}} \\ &+ \underbrace{\mathbb{E}[D_{\text{KL}}(f_{\text{dis}}(z^*) || \mathcal{U}(z^*))]}_{\text{For } \mathcal{E}}, \end{aligned} \quad (8)$$

where o^* is pseudo labels generated by a student model for representing whether the latent feature belongs to which domain *e.g.*, When z^s is given, o^s is set by 0. $\mathcal{U}(z^*)$ represents a vector to define a uniform distribution having the same dimensionality with z^* . In this work, since our adversarial learning is formulated based on the three classes, *i.e.*, $\mathcal{U}(z^*)$ is defined by the three-dimensional vector initialised by 1/3 for each element.

3.5. Training and Inference

We conduct pre-training and fine-tuning to optimise the CICLD for unsupervised domain adaptive semantic segmentation. The pre-training is essential for diffusion-based segmentation, which is very slow to optimise the model. Also,

we optimise the model parameters to fit the model to the unsupervised domain adaptive semantic segmentation by producing the fine-tuning task. After finishing all training steps, the student model is used for the semantic segmentation model for the target domain. A detailed explanation of those training and inference tasks is below.

Pre-training: The pre-training involves a two-stage approach, each utilizing specific loss functions to achieve high-quality and efficient image synthesis. In the first stage, an autoencoder is trained to compress high-dimensional image data into a lower-dimensional latent space while preserving the perceptual quality of the images. This is achieved through a combination of loss functions: the perceptual loss ensures that the reconstructed image retains the high-level features of the original image by comparing features extracted from a pre-trained network, the patch-based adversarial loss promotes the generation of locally realistic image patches by using a discriminator, and regularisation losses—such as KL divergence and vector quantisation—structure the latent space to ensure meaningful representations. The total loss function for the autoencoder is a weighted combination of these components, balancing the contributions of perceptual, adversarial, and regularisation losses. In the second stage, the diffusion model is trained within the latent space created by the autoencoder. This step leverages the latent space’s reduced dimensionality to make training and inference more efficient. The diffusion model uses a time-conditional UNet architecture and is trained with a reweighted variational objective, which aims to predict the noise added to the latent representation at each timestep. This loss function measures the mean squared error between the predicted and actual noise, guiding the model to effectively denoise progressively noisier latent representations. These loss functions enable LDMs to produce high-resolution, high-fidelity images with significantly reduced computational requirements.

Fine-tuning: After the initial pre-training phase involving the autoencoder and diffusion model in the latent space, Latent Diffusion Models (LDMs) undergo further training to enhance their generative capabilities and adapt to various conditional tasks. This stage leverages flexible conditioning mechanisms, such as cross-attention layers and concatenation, which allow the model to incorporate additional information like text descriptions, semantic maps, or low-resolution images. Cross-attention layers enable the model to focus on relevant parts of the conditioning input by computing attention scores, while concatenation provides direct access to conditioning information. The primary loss function remains similar to the reweighted variational objective used during pre-training. Still, it is adapted to include the conditioning inputs, guiding the model to generate images that match the conditioning input with high fidelity. Task-specific losses, such as perceptual

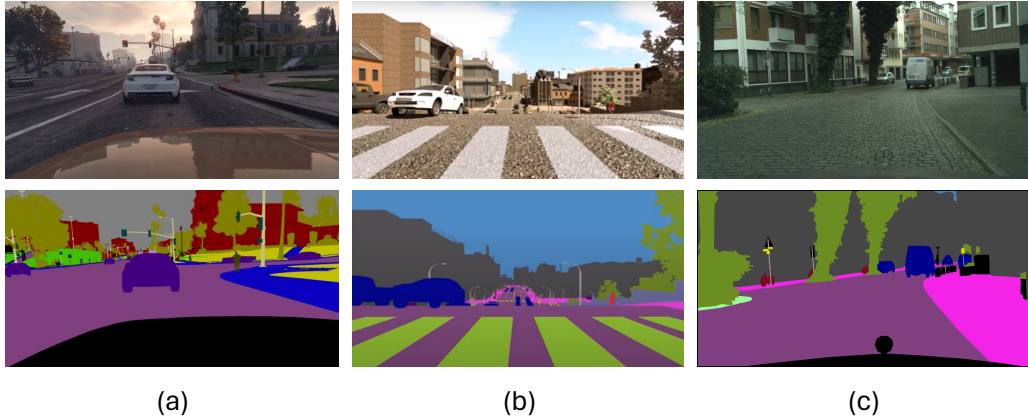


Figure 3: Example images and labels of the (a) GTA-5 [3], (b) SYNTHIA [4], and (c) Cityscapes datasets [5].

loss, pixel-wise L2 loss, and adversarial loss, are used for applications like super-resolution, inpainting, and text-to-image synthesis to ensure sharp, realistic outputs. Fine-tuning involves hyperparameter adjustments, evaluation using metrics like FID (Fréchet inception distance), IS (inception score), PSNR (peak signal to noise ratio), and SSIM (structural similarity index measure), and implementing efficient sampling techniques like DDIM to optimize performance and speed up the generation process. Further training is crucial for achieving state-of-the-art performance across various image synthesis tasks while maintaining computational efficiency.

Inference: After finishing all the training steps, the inference is straightforwardly conducted with the student model. As shown in Fig. 1, the teacher model, which is a segmentation model for the source and mixed domain, will not be used for inference. The student model optimised by the EMA algorithm and the teacher model will work to obtain segmentation results for the target domain. This inference task is a typical approach for the UDA using a teacher-student learning process. During the performance evaluation, all figures were obtained by the student model.

4. Experimental settings

4.1. Experiment details

We choose **GTA5** [3], **SYNTHIA** [4], **Cityscapes** [5] datasets for our experiments. Those datasets are publicly available. Fig 3 shows the example snapshots of images and labels of those three datasets. Detailed information on those datasets is as follows.

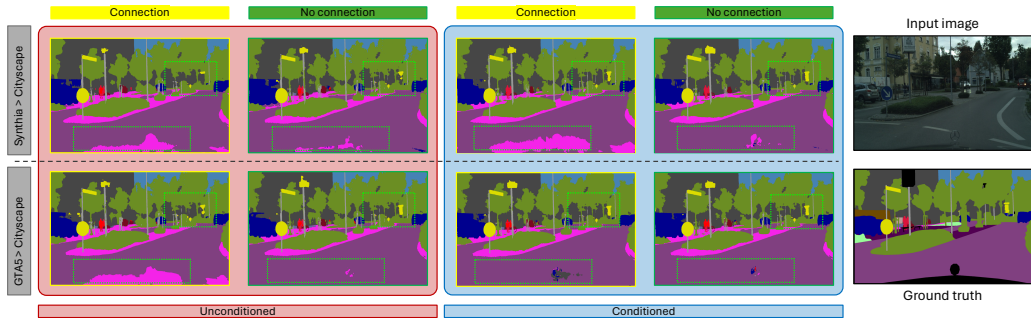


Figure 4: Qualitative comparison of the UDA performance with the proposed method with other methods. The results on $\text{GTA} \rightarrow \text{Cityscapes}$ note that the proposed method shows performance improvement in classes like Sidewalk, Fence, Bus, etc, highlighted using dotted boxes compared with other methods.

GTA-5¹ has 24,966 synthetic images extracted from a photo-realistic open-world game called Grand Theft Auto, along with semantic segmentation maps. The image resolution is 1914×1052 .

Synthia² is a synthetic dataset comprising 9400 photo-realistic frames with a resolution of 1280×960 , rendered from a virtual city with pixel-level annotations for 13 classes.

Cityscapes³ is a large-scale database that focuses on semantic understanding of urban street scenes. The dataset has semantically annotated 2975 training images and 500 validation images with a resolution of 2048×1024 .

We evaluate the UDA performances for GTA5 and Synthia to Cityscape using the above dataset. The experiment protocol is referred from the CLUDA [15] and Toldo *et al.* [48].

We use the Latent Diffusion Model (LDM) [43] as the backbone. The LDM uses UNet structure [25] so that the neural network components for applying adversarial learning are also built based on the encoding part of the UNet with the two extra fully connected networks with the dimensionalities of 1024 and 3 for the classification tasks. The Adam optimiser is used to train the three components. The initial learning rate is 6×10^{-5} , and the learning rate is decayed every five

¹https://download.visinf.tu-darmstadt.de/data/from_games

²<https://synthia-dataset.net/>

³<https://www.cityscapes-dataset.com/>

epochs by multiplying 0.99 by the learning rate. The batch size is 2. Fifty epochs are set for training. For updating the student model, we keep the value of EMA weight update parameter $\alpha = 0.999$; for learning-rate optimisation, we follow polynomial-learning rate reduction⁴.

5. Ablation study

5.1. Effectiveness of the conditioning

We built the conditioning module to improve the contextual property when a given latent feature is being denoised and transferred for semantic segmentation, and it is one of the key differences between our method and other diffusion-based segmentation methods [34, 35, 36, 37, 43].

To demonstrate the effectiveness of the conditioning module for semantic segmentation using the diffusion model, we conduct ablation studies by comparing the segmentation performances depending on the usage of the conditioning module.

Table 1 shows the segmentation performances for the models taking the conditioning module and without the module. The segmentation obtained with the conditioning module achieves 74.4 mIoU for the GTA5 \rightarrow Cityscape UDA setting. Those figures are 5.1% higher than the performances of the model without the conditioning module. In the Synthia \rightarrow Cityscape UDA setting, the segmentation obtained with the conditioning module achieves 67.2 of mIoU. The segmentation performance without the conditioning module shows 69.3 mIoU and 58.5 mIoU for the GTA5 \rightarrow Cityscape UDA and Synthia \rightarrow Cityscape UDA settings, respectively.

Those results are also represented in the qualitative results in Fig. 4; the segmentation results of the model using the conditioning module provide more distinguishing results (See the yellow coloured box areas). The quantitative and qualitative results demonstrate that the conditioning module helps improve the segmentation performance in the UDA setting.

5.2. Effectiveness of the inter-coder connection

The inter-coder connection is built to bring the wide range of latent features available from the encoder’s feature extraction process to the decoder. The inter-coder connection is motivated by the skip connection on the UNet [56] and ResNet [2] so we expected to improve the feature representation performance by concatenating the low-level and high-level latent features from the encoder to improve the

⁴This project is publicly available on <https://github.com/andreYoo/CICLD>

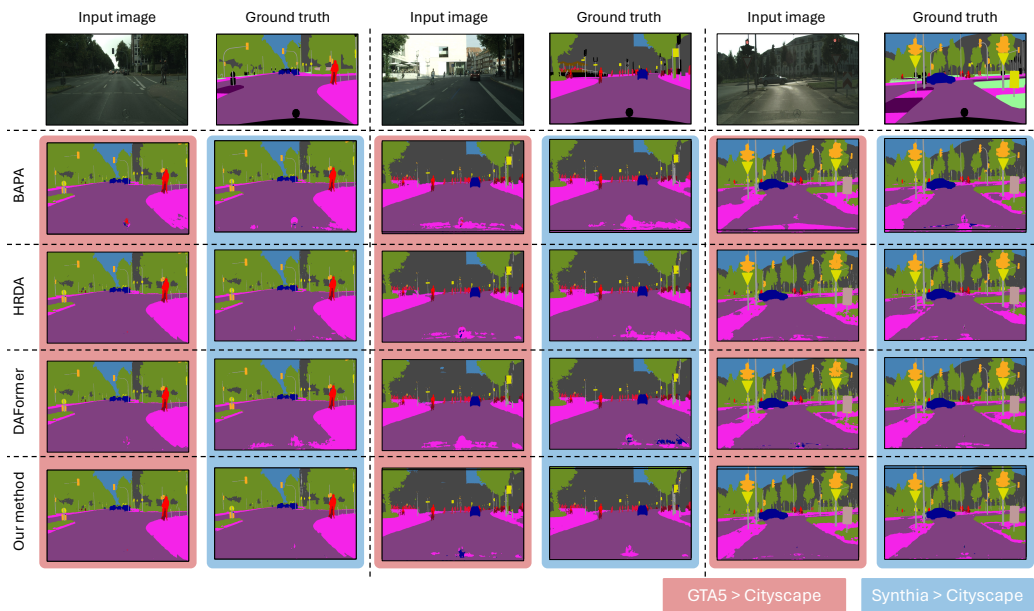


Figure 5: Qualitative comparison of the UDA performance with the proposed method with HRDA [55], DAFormer [19], and BAPA [53]. HRDA and DAFormer achieve the 2nd and 3th ranked performances based on mIoU (See Table 3), and BAPA produces the best performance for the Veget classes on the Synthia \rightarrow Cityscape UDA setting. The visualisation of the segmentation results show that the proposed method produces more precise segmentation performance than the other methods.

UDA settings	GTA5 \rightarrow Cityscape	Synthia \rightarrow Cityscape
Without the Inter-coder connection		
Unconditioned	58.3	42.7
Conditioned	69.3	58.5
With the Inter-coder connection		
Unconditioned	68.4	60.7
Conditioned	74.4	67.2

Table 1: Quantitative results depending on the usages of the conditioning module and the inter-coder connection. The lined figure denotes the lowest performance, and the numbers and the arrow marks inside the bracket denote the performance gap from the lowest one. The bolded figure defines the best performance among the results.

precision in predicting the pixel-level segmentation results. This connection is a key structural difference between our architecture and LDM.

To demonstrate the effectiveness of the inter-coder connection, we built two segmentation models. One has an inter-coder connection, and the other one has no inter-coder connection. The dimensionalities of the hidden layers on the decoder of the model without the inter-coder connection are relatively smaller than the model with the inter-coder connection because the input of each decoder layer has no features bridged from the encoder. Table 1 also shows the segmentation performance of the two models on the GTA to Cityscape and Synthai to Cityscape UDA setting. Fig. 4 includes the segmentation results for the UDA settings.

The segmentation model, by using the inter-coder connection, achieves 74.4 of mIoU for the GTA5 \rightarrow Cityscape UDA setting. Also, the model produces 69.3 mIoU for the Synthia \rightarrow Cityscape UDA setting. The model without the connection produces 69.3 mIoU for the GTA5 \rightarrow Cityscape UDA setting. Also, the model produces 58.3 mIoU for the Synthia \rightarrow Cityscape UDA setting, which performs less than the model, including the connection. The quantitative results in Fig. 4 also show that the model, including the connection, predicts more precise segmentation results. In particular, in predicting the object boundaries, the model with the connection performs better than the other. Consequently, overall results justify that the inter-coder connection helps improve the segmentation performance on our architecture settings.

Loss function	Objective settings										
\mathcal{L}_{Cls}	✓	✓	✓	✓	✓	✓	✓	✓	✓	✓	✓
2 classes \mathcal{L}_{Adv} [49]		✓					✓		✓		✓
3 classes \mathcal{L}_{Adv} (Ours)			✓					✓		✓	✓
CL [15]				✓		✓	✓			✓	✓
MMD [50]					✓				✓	✓	✓
mIoU _{G2C}	42.8	65.7	74.4	71.6	64.2	73.1	74.9	70.3	71.6	64.8	70.5
mIoU _{S2C}	31.6	54.1	67.2	60.3	48.6	62.5	68.1	58.7	60.1	58.2	59.9

Table 2: Quantitative results of the UDA performances depending on the objective function settings. The CL and MMD stand for contrastive learning [15] and maximum mean discrepancy [50]. mIoU_{G2C} and mIoU_{S2C} denote that the averaged Intersection of Union (mIoU) for the GTA5 → Cityscape UDA setting and the Synthia → Cityscape UDA setting, respectively. The bolded figure denotes the best results, and it is achieved by the combination of \mathcal{L}_{Cls} , 3 classes \mathcal{L}_{Adv} , and the CL [15]. The bolded figures represent the best performance.

5.3. Effectiveness of \mathcal{L}_{Adv}

We formulate adversarial learning using cross-entropy and KL-divergence to explicitly align the latent feature distributions for the source and target domains. Unlike other UDA methods using adversarial learning, which apply the adversarial learning strategy for the source and target domain only, our adversarial learning takes three domains *i.e.*, the source, mixed, and target domains, so that, rather than computing the cross-entropy loss with the fake labels about the target domains for updating the encoder, our adversarial learning tries to minimise the KL-divergence between the classification likelihood and the uniform distribution.

We conducted ablation studies to demonstrate the effectiveness of adversarial learning. Table 2 shows the segmentation performances depending on the loss function settings. We not only compare the segmentation performance depending on the usage of adversarial learning but also compare the segmentation performance with other adversarial and contrastive learning-based UDA methods [49, 15, 50]. The experimental results demonstrate the effectiveness of adversarial learning. The models trained with objective functions with the proposed adversarial loss always perform better than those trained with the loss functions, considering the two classes of adversarial loss. The best performance was achieved by the model

Method	mIoU	Road	S.Walk	Build.	Wall	Fence	Pole	T. Light	T. Sign	Veget.	Terrain	Sky	Person	Rider	Car	Truck	Bus	Train	M.Bike	Bike
GTAS → Cityscapes																				
AdaptSeg[17]	41.4	86.5	25.9	79.8	22.1	20.0	23.6	33.1	21.8	81.8	25.9	75.9	57.3	26.2	76.3	29.8	32.1	7.2	29.5	32.5
CBST[18]	45.9	91.8	53.5	80.5	32.7	21.0	34.0	28.9	20.4	83.9	34.2	80.9	53.1	24.0	82.7	30.3	35.9	16.0	25.9	42.8
DACS[51]	52.1	89.9	39.7	87.9	30.7	39.5	38.5	46.4	52.8	88.0	44.0	88.8	67.2	35.8	84.5	45.7	50.2	0.0	27.3	34.0
CorDA[52]	56.6	94.7	63.1	87.6	30.7	40.6	40.2	47.8	51.6	87.6	47.0	89.7	66.7	35.9	90.2	48.9	57.5	0.0	39.8	56.0
BAPA[53]	57.4	94.4	61.0	88.0	26.8	39.9	38.3	46.1	55.3	87.8	46.1	89.4	68.8	40.0	90.2	60.4	59.0	0.0	45.1	54.2
ProDA[54]	57.5	87.8	56.0	79.7	46.3	44.8	45.6	53.5	53.5	88.6	45.2	82.1	70.7	39.2	88.8	45.5	59.4	1.0	48.9	56.4
DAFormer[19]	68.3	95.7	70.2	89.4	53.5	48.1	49.6	55.8	59.4	89.9	47.9	92.5	72.2	44.7	92.3	74.5	78.2	65.1	55.9	61.8
HRDA [55]	73.8	96.4	74.4	91.0	61.6	51.5	57.1	63.9	69.3	91.3	48.4	94.2	79.0	52.9	93.9	84.1	85.7	75.9	63.9	67.5
Our method	74.4	97.6	74.3	90.9	62.3	52.3	57.0	64.9	72.5	91.1	51.3	94.5	78.6	53.2	94.5	84.9	85.4	75.1	65.4	66.7
Synthia → Cityscapes																				
AdaptSeg[17]	37.2	79.2	37.2	78.8	-	-	-	9.9	10.5	78.2	-	80.5	53.5	19.6	67.0	-	29.5	-	21.6	31.3
CBST[18]	42.6	68.0	29.9	76.3	10.8	1.4	33.9	22.8	29.5	77.6	-	78.3	60.6	28.3	81.6	-	23.5	-	18.8	39.8
DACS[51]	48.3	80.6	25.1	81.9	21.5	2.9	37.2	22.7	24.0	83.7	-	90.8	67.5	38.3	82.9	-	38.9	-	28.5	47.6
CorDA[52]	55.0	93.3	61.6	85.3	19.6	5.1	37.8	36.6	42.8	84.9	-	90.4	69.7	41.8	85.6	-	38.4	-	32.6	53.9
BAPA[53]	53.3	91.7	53.8	83.9	22.4	0.8	34.9	30.5	42.8	86.8	-	88.2	66.0	34.1	86.6	-	51.3	-	29.4	50.5
ProDA[54]	55.0	93.3	61.6	85.3	19.6	5.1	37.8	36.6	42.8	84.9	-	90.4	69.7	41.8	85.6	-	38.4	-	32.6	53.9
DAFormer[19]	60.9	84.5	40.7	88.4	41.5	6.5	50.0	55.0	54.6	86.0	-	89.8	73.2	48.2	87.2	-	53.2	-	53.9	61.7
HRDA [55]	65.8	85.2	47.7	88.8	49.5	4.8	57.2	65.7	60.9	85.3	-	92.9	79.4	52.8	89.0	-	64.7	-	63.9	64.9
Our method	67.2	91.3	48.5	89.9	49.5	8.5	58.6	67.4	60.2	86.2	-	93.4	79.8	54.2	88.9	-	66.7	-	65.5	65.7

Table 3: Comparison with state-of-the-art methods for UDA. The bolded figures represent the best performances.

trained with objective functions, including proposed adversarial learning, cross-entropy loss, and conservative learning loss [15]. We can observe that the model’s performance using the proposed adversarial learning improves the segmentation performance constantly, and the results are even better than the normal adversarial learning loss.

When analysing the performance metrics, the 3 Class \mathcal{L}_{Adv} (Ours) setting consistently outperforms the 2 Class adversarial loss [49] baseline across both mIoU $_{G2C}$ and mIoU $_{S2C}$ metrics. For instance, in the context of mIoU $_{G2C}$, the 3 Class \mathcal{L}_{Adv} setting achieves scores as high as 74.9, compared to the maximum score of 73.1 under the 2 Class \mathcal{L}_{Adv} setup. Similarly, for mIoU $_{S2C}$, the 3 Class \mathcal{L}_{Adv} setting reaches peak performance of 68.1, whereas the 2 Class \mathcal{L}_{Adv} setting lags behind with a maximum of 62.5. These results underscore the superiority of the 3-class adversarial loss in improving the model’s accuracy and reliability.

Moreover, the consistent performance improvements observed with the 3 Class \mathcal{L}_{Adv} across different configurations suggest that this setting is more robust and versatile. The increased complexity introduced by the three-class adversarial loss likely helps the model learn more discriminative features and better adapt to variations in the data, resulting in higher mIoU scores.

6. Comparison with existing UDA methods

We begin by comparing the proposed approach with existing UDA methods [17, 18, 51, 52, 53, 54, 19, 55]. We show that our method achieves better performance than the current state-of-the-art methods by a margin of +0.6 mIoU in GTA5 \rightarrow Cityscapes and +1.4 mIoU in Synthia \rightarrow Cityscapes in Table 3. Class-wise improvements can be seen in 11 of the 19 classes in GTA5 \rightarrow Cityscapes, where major improvements can be seen in difficult classes like Wall, Rider, Fence, etc., and 12 of the 16 classes in Synthia \rightarrow Cityscapes, as also supported quantitatively in Table 3.

The proposed method achieves 74.4 mIoU for the GTA5 \rightarrow Cityscapes UDA setting and 67.2 mIoU for the Synthia \rightarrow Cityscapes UDA setting. Overall, the proposed method outperforms the other methods. However, the HRDA [55] performs better in the GTA5 \rightarrow Cityscapes UDA settings in some particular classes. The HRDA [55] achieves better performances for the sidewalk (S.Walk), building (Build), pole, vegetation (Veget), person, bus, train, and bike. In the Synthia \rightarrow Cityscapes UDA results, BAPA [53] and HRAD [55] show better performance for some particular classes. The BAPA [53] produces 86.8 IoU for the Veget class, and the HRDA achieves 60.9 IoU and 89.0 IoU for the traffic sign (T. Sign) and car, respectively. However, the performance gap between those methods and our method is usually less than 0.2, suggesting that the proposed method also achieves very competitive performance for the above classes.

We not only compare the quantitative results but also the qualitative results. Fig. 5 shows the segmentation results of the proposed method and some methods achieving comparable performance with ours. HRDA [55] and DAFormer [19] are selected because those methods produce 2nd and 3th ranked performances based on mIoU. We also show the visualisation results of the UDA segmentation results using BAPA [53] since it produces the best performance for the Veget class on the Synthia \rightarrow Cityscape UDA setting (86.8 IoU, see Table. 3). The visualisation results show that the proposed method produces less noisy segmentation results for both UDA settings, which can be interpreted as our method can have a more generalised representation from a source domain.

7. Conclusion

In this paper, we propose a Conditional and Inter-coder Connected Latent Diffusion (CICLD) for unsupervised domain adaptive semantic segmentation. The CICLD, leverages latent diffusion models (LDMs) and adversarial learning to

enhance the generalisation capability of semantic segmentation models across different domains. The key contributions include the conditioning module, which enhances generalisation by modelling gradual transitions between domains and improving segmentation accuracy through a conditioning mechanism for segmentation masks. The Inter-coder Connection is a structural innovation that preserves fine-grained details and spatial hierarchies, crucial for precise semantic segmentation. The adversarial learning component explicitly aligns latent feature distributions from source, mixed, and target domains, enhancing the model’s ability to generalise across different domains with a novel three-class adversarial loss. Experimental results demonstrate that CICLD significantly outperforms state-of-the-art UDA methods on benchmarks such as GTA5 to Cityscapes and Synthia to Cityscapes, with notable improvements in mean Intersection over Union (mIoU) scores, particularly in challenging classes like walls, riders, and fences. The model achieved 74.4 mIoU for the GTA5 to Cityscapes UDA setting and 67.2 mIoU for the Synthia to Cityscapes UDA setting, surpassing existing methods. Overall, CICLD presents a robust and innovative solution for unsupervised domain adaptation in semantic segmentation, showing considerable potential for real-world applications by effectively handling domain variations and improving segmentation model performance in diverse environments.

However, even though the proposed method shows outstanding performance compared with the existing state-of-the-art methods, there is a critical drawback which has to be resolved in the future. The huge, time-consuming diffusion process is it. Our method contains the noising and denoising process for the diffusion model, and, this process is very time-consuming. Additionally, the performance, depending on the number of sampling steps, is a critical issue. This issue is a common problem in all studies leveraging diffusion models. In conclusion, our method has shown promising results, but there is room for improvement in computational complexity and processing speed. Our future research will focus on optimising the algorithm and exploring more efficient techniques to develop a more robust and scalable solution for UDA tasks.

References

- [1] K. He, X. Chen, S. Xie, Y. Li, P. Dollár, R. Girshick, Masked autoencoders are scalable vision learners, in: Proceedings of the IEEE/CVF conference on computer vision and pattern recognition, 2022, pp. 16000–16009.
- [2] K. He, X. Zhang, S. Ren, J. Sun, Deep residual learning for image recognition,

- in: Proceedings of the IEEE conference on computer vision and pattern recognition, 2016, pp. 770–778.
- [3] S. R. Richter, V. Vineet, S. Roth, V. Koltun, Playing for data: Ground truth from computer games, in: European conference on computer vision, Springer, 2016, pp. 102–118.
 - [4] G. Ros, L. Sellart, J. Materzynska, D. Vazquez, A. M. Lopez, The synthia dataset: A large collection of synthetic images for semantic segmentation of urban scenes, in: Proceedings of the IEEE conference on computer vision and pattern recognition, 2016, pp. 3234–3243.
 - [5] M. Cordts, M. Omran, S. Ramos, T. Rehfeld, M. Enzweiler, R. Benenson, U. Franke, S. Roth, B. Schiele, The cityscapes dataset for semantic urban scene understanding, in: Proceedings of the IEEE conference on computer vision and pattern recognition, 2016, pp. 3213–3223.
 - [6] Y. Li, L. Yuan, N. Vasconcelos, Bidirectional learning for domain adaptation of semantic segmentation, in: Proceedings of the IEEE/CVF conference on computer vision and pattern recognition, 2019, pp. 6936–6945.
 - [7] J. Wang, Z. Zheng, A. Ma, X. Lu, Y. Zhong, Loveda: A remote sensing land-cover dataset for domain adaptive semantic segmentation, arXiv preprint arXiv:2110.08733 (2021).
 - [8] G. French, S. Laine, T. Aila, M. Mackiewicz, G. Finlayson, Semi-supervised semantic segmentation needs strong, varied perturbations, arXiv preprint arXiv:1906.01916 (2019).
 - [9] L. Hoyer, D. Dai, Y. Chen, A. Koring, S. Saha, L. Van Gool, Three ways to improve semantic segmentation with self-supervised depth estimation, in: Proceedings of the IEEE/CVF Conference on Computer Vision and Pattern Recognition, 2021, pp. 11130–11140.
 - [10] X. Lai, Z. Tian, L. Jiang, S. Liu, H. Zhao, L. Wang, J. Jia, Semi-supervised semantic segmentation with directional context-aware consistency, in: Proceedings of the IEEE/CVF Conference on Computer Vision and Pattern Recognition, 2021, pp. 1205–1214.

- [11] N. Souly, C. Spampinato, M. Shah, Semi supervised semantic segmentation using generative adversarial network, in: Proceedings of the IEEE international conference on computer vision, 2017, pp. 5688–5696.
- [12] J. Dai, K. He, J. Sun, Boxsup: Exploiting bounding boxes to supervise convolutional networks for semantic segmentation, in: Proceedings of the IEEE international conference on computer vision, 2015, pp. 1635–1643.
- [13] C. Song, Y. Huang, W. Ouyang, L. Wang, Box-driven class-wise region masking and filling rate guided loss for weakly supervised semantic segmentation, in: Proceedings of the IEEE/CVF Conference on Computer Vision and Pattern Recognition, 2019, pp. 3136–3145.
- [14] Y. Zou, Z. Zhang, H. Zhang, C.-L. Li, X. Bian, J.-B. Huang, T. Pfister, Pseudoseg: Designing pseudo labels for semantic segmentation, arXiv preprint arXiv:2010.09713 (2020).
- [15] M. Vayyat, J. Kasi, A. Bhattacharya, S. Ahmed, R. Tallamraju, Cluda: Contrastive learning in unsupervised domain adaptation for semantic segmentation, arXiv preprint arXiv:2208.14227 (2022).
- [16] J. Hoffman, D. Wang, F. Yu, T. Darrell, Fcns in the wild: Pixel-level adversarial and constraint-based adaptation, arXiv preprint arXiv:1612.02649 (2016).
- [17] Y.-H. Tsai, W.-C. Hung, S. Schuler, K. Sohn, M.-H. Yang, M. Chandraker, Learning to adapt structured output space for semantic segmentation, in: Proceedings of the IEEE conference on computer vision and pattern recognition, 2018, pp. 7472–7481.
- [18] Y. Zou, Z. Yu, B. Kumar, J. Wang, Unsupervised domain adaptation for semantic segmentation via class-balanced self-training, in: Proceedings of the European conference on computer vision (ECCV), 2018, pp. 289–305.
- [19] L. Hoyer, D. Dai, L. Van Gool, Daformer: Improving network architectures and training strategies for domain-adaptive semantic segmentation, arXiv preprint arXiv:2111.14887 (2021).
- [20] J. Yu, H. Oh, S. Fichera, P. Paoletti, S. Luo, Multi-source domain adaptation for unsupervised road defect segmentation, in: 2023 IEEE International

- Conference on Robotics and Automation (ICRA), IEEE, 2023, pp. 5638–5644.
- [21] C.-X. Ren, P. Ge, P. Yang, S. Yan, Learning target-domain-specific classifier for partial domain adaptation, *IEEE Transactions on Neural Networks and Learning Systems* 32 (5) (2020) 1989–2001.
 - [22] J. Yu, H. Oh, J. Yang, Adversarial denoising diffusion model for unsupervised anomaly detection, in: *Deep Generative Models for Health Workshop NeurIPS 2023*, 2023.
 - [23] J. Ho, A. Jain, P. Abbeel, Denoising diffusion probabilistic models, *Advances in neural information processing systems* 33 (2020) 6840–6851.
 - [24] E. Xie, W. Wang, Z. Yu, A. Anandkumar, J. M. Alvarez, P. Luo, Segformer: Simple and efficient design for semantic segmentation with transformers, *Advances in neural information processing systems* 34 (2021) 12077–12090.
 - [25] O. Ronneberger, P. Fischer, T. Brox, U-net: Convolutional networks for biomedical image segmentation, in: *Medical image computing and computer-assisted intervention–MICCAI 2015: 18th international conference, Munich, Germany, October 5-9, 2015, proceedings, part III* 18, Springer, 2015, pp. 234–241.
 - [26] J. Chen, Y. Lu, Q. Yu, X. Luo, E. Adeli, Y. Wang, L. Lu, A. L. Yuille, Y. Zhou, Transunet: Transformers make strong encoders for medical image segmentation, *arXiv preprint arXiv:2102.04306* (2021).
 - [27] R. Strudel, R. Garcia, I. Laptev, C. Schmid, Segformer: Transformer for semantic segmentation, in: *Proceedings of the IEEE/CVF international conference on computer vision*, 2021, pp. 7262–7272.
 - [28] Y. LeCun, B. Boser, J. Denker, D. Henderson, R. Howard, W. Hubbard, L. Jackel, Handwritten digit recognition with a back-propagation network, *Advances in neural information processing systems* 2 (1989).
 - [29] R. Ranftl, A. Bochkovskiy, V. Koltun, Vision transformers for dense prediction, in: *Proceedings of the IEEE/CVF international conference on computer vision*, 2021, pp. 12179–12188.

- [30] E. Kats, J. G. Hirsch, M. P. Heinrich, Self-supervised learning of dense hierarchical representations for medical image segmentation, arXiv preprint arXiv:2401.06473 (2024).
- [31] M. Seince, L. Le Folgoc, L. F. De Souza, E. Angelini, Dense self-supervised learning for medical image segmentation, in: *Medical Imaging with Deep Learning*, 2024.
- [32] Y. Song, J. Sohl-Dickstein, D. P. Kingma, A. Kumar, S. Ermon, B. Poole, Score-based generative modeling through stochastic differential equations, arXiv preprint arXiv:2011.13456 (2020).
- [33] J. Song, C. Meng, S. Ermon, Denoising diffusion implicit models, arXiv preprint arXiv:2010.02502 (2020).
- [34] D. Baranchuk, I. Rubachev, A. Voynov, V. Khrukov, A. Babenko, Label-efficient semantic segmentation with diffusion models, arXiv preprint arXiv:2112.03126 (2021).
- [35] H. Tan, S. Wu, J. Pi, Semantic diffusion network for semantic segmentation, *Advances in Neural Information Processing Systems* 35 (2022) 8702–8716.
- [36] W. Wu, Y. Zhao, M. Z. Shou, H. Zhou, C. Shen, Diffumask: Synthesizing images with pixel-level annotations for semantic segmentation using diffusion models, in: *Proceedings of the IEEE/CVF International Conference on Computer Vision*, 2023, pp. 1206–1217.
- [37] T. Amit, T. Shaharbany, E. Nachmani, L. Wolf, Segdiff: Image segmentation with diffusion probabilistic models, arXiv preprint arXiv:2112.00390 (2021).
- [38] W. Wang, X. Yu, B. Fang, Y. Zhao, Y. Chen, W. Wei, J. Chen, Cross-modality lge-cmr segmentation using image-to-image translation based data augmentation, *IEEE/ACM Transactions on Computational Biology and Bioinformatics* 20 (4) (2022) 2367–2375.
- [39] J. Hoffman, E. Tzeng, T. Park, J.-Y. Zhu, P. Isola, K. Saenko, A. Efros, T. Darrell, Cycada: Cycle-consistent adversarial domain adaptation, in: *International conference on machine learning*, Pmlr, 2018, pp. 1989–1998.
- [40] K. Saito, S. Yamamoto, Y. Ushiku, T. Harada, Adversarial learning approach for open set domain adaptation, in: *Domain Adaptation in Computer Vision with Deep Learning*, Springer, 2020, pp. 175–193.

- [41] Y. Zhang, P. David, B. Gong, Curriculum domain adaptation for semantic segmentation of urban scenes, in: Proceedings of the IEEE international conference on computer vision, 2017, pp. 2020–2030.
- [42] V. Olsson, W. Tranheden, J. Pinto, L. Svensson, Classmix: Segmentation-based data augmentation for semi-supervised learning, in: Proceedings of the IEEE/CVF Winter Conference on Applications of Computer Vision, 2021, pp. 1369–1378.
- [43] R. Rombach, A. Blattmann, D. Lorenz, P. Esser, B. Ommer, High-resolution image synthesis with latent diffusion models, in: Proceedings of the IEEE/CVF conference on computer vision and pattern recognition, 2022, pp. 10684–10695.
- [44] A. Krizhevsky, I. Sutskever, G. E. Hinton, Imagenet classification with deep convolutional neural networks, Communications of the ACM 60 (6) (2017) 84–90.
- [45] M. Drozdal, E. Vorontsov, G. Chartrand, S. Kadoury, C. Pal, The importance of skip connections in biomedical image segmentation, in: International workshop on deep learning in medical image analysis, international workshop on large-scale annotation of biomedical data and expert label synthesis, Springer, 2016, pp. 179–187.
- [46] Z. Huang, P. Zhou, S. Yan, L. Lin, Scalelong: Towards more stable training of diffusion model via scaling network long skip connection, Advances in Neural Information Processing Systems 36 (2023) 70376–70401.
- [47] C. Szegedy, V. Vanhoucke, S. Ioffe, J. Shlens, Z. Wojna, Rethinking the inception architecture for computer vision, in: Proceedings of the IEEE conference on computer vision and pattern recognition, 2016, pp. 2818–2826.
- [48] M. Toldo, U. Michieli, P. Zanuttigh, Unsupervised domain adaptation in semantic segmentation via orthogonal and clustered embeddings, in: Proceedings of the IEEE/CVF Winter conference on Applications of Computer Vision, 2021, pp. 1358–1368.
- [49] E. Tzeng, J. Hoffman, K. Saenko, T. Darrell, Adversarial discriminative domain adaptation, in: Proceedings of the IEEE conference on computer vision and pattern recognition, 2017, pp. 7167–7176.

- [50] M. Long, Y. Cao, J. Wang, M. Jordan, Learning transferable features with deep adaptation networks, in: International conference on machine learning, PMLR, 2015, pp. 97–105.
- [51] W. Tranheden, V. Olsson, J. Pinto, L. Svensson, Dacs: Domain adaptation via cross-domain mixed sampling, in: Proceedings of the IEEE/CVF Winter Conference on Applications of Computer Vision, 2021, pp. 1379–1389.
- [52] Q. Wang, D. Dai, L. Hoyer, L. Van Gool, O. Fink, Domain adaptive semantic segmentation with self-supervised depth estimation, in: Proceedings of the IEEE/CVF International Conference on Computer Vision, 2021, pp. 8515–8525.
- [53] Y. Liu, J. Deng, X. Gao, W. Li, L. Duan, Bapa-net: Boundary adaptation and prototype alignment for cross-domain semantic segmentation, in: Proceedings of the IEEE/CVF International Conference on Computer Vision, 2021, pp. 8801–8811.
- [54] P. Zhang, B. Zhang, T. Zhang, D. Chen, Y. Wang, F. Wen, Prototypical pseudo label denoising and target structure learning for domain adaptive semantic segmentation, in: Proceedings of the IEEE/CVF Conference on Computer Vision and Pattern Recognition, 2021, pp. 12414–12424.
- [55] L. Hoyer, D. Dai, L. Van Gool, Hrda: Context-aware high-resolution domain-adaptive semantic segmentation, arXiv preprint arXiv:2204.13132 (2022).
- [56] W. Weng, X. Zhu, Inet: convolutional networks for biomedical image segmentation, Ieee Access 9 (2021) 16591–16603.